Hindawi
Journal of Nanomaterials
Volume 2017, Article ID 7359591, 11 pages
https://doi.org/10.1155/2017/7359591

Research Article

Impact on CO_2 Uptake of MWCNT after Acid Treatment Study

Michal Zgrzebnicki, Nikola Krauze, Andżelika Gęsikiewicz-Puchalska, Joanna Kapica-Kozar, Ewa Piróg, Anna Jędrzejewska, Beata Michalkiewicz, Urszula Narkiewicz, Antoni W. Morawski, and Rafal J. Wrobel

Faculty of Chemical Technology and Engineering, West Pomeranian University of Technology Szczecin, Institute of Chemical and Environment Engineering, Pułaskiego 10, 70–322 Szczecin, Poland

Correspondence should be addressed to Rafal J. Wrobel; rwrobel@zut.edu.pl

Received 24 May 2017; Revised 9 August 2017; Accepted 29 August 2017; Published 11 October 2017

Academic Editor: Ester Vazquez

Greenhouse effect is responsible for keeping average temperature of Earth's atmosphere at level of about 288 K. Its intensification leads to warming of our planet and may contribute to adverse changes in the environment. The most important pollution intensifying greenhouse effect is anthropogenic carbon dioxide. This particular gas absorbs secondary infrared radiation, which in the end leads to an increase of average temperature of Earth's atmosphere. Main source of CO_2 is burning of fossil fuels, like oil, natural gas, and coal. Therefore, to reduce its emission, a special CO_2 capture and storage technology is required. Carbonaceous materials are promising materials for CO_2 sorbents. Thus multiwalled carbon nanotubes, due to the lack of impurities like ash in activated carbons, were chosen as a model material for investigation of acid treatment impact on CO_2 uptake. Remarkable 43% enhancement of CO_2 sorption capacity was achieved at 273 K and relative pressure of 0.95. Samples were also thoroughly characterized in terms of texture (specific surface area measurement, transmission electron microscope) and chemical composition (X-ray photoelectron spectroscopy).

1. Introduction

It has been observed during the last 60 years of continuous measurements that concentration of CO_2 in the atmosphere is steadily increasing [1]. According to the obtained data, concentration of this particular greenhouse gas was about 315 ppm in March 1958 and in November 2016 reached 404 ppm [2]. Compared to preindustrial revolution level, that is, 280 ppm, it is almost a 50% increase of carbon dioxide concentration [3]. Simultaneously the average temperature of atmosphere is increasing [1]. According to NASA's Goddard Institute for Space Studies (GISS) [4], the highest temperature increase was observed in 2015. It was an increase of 0.87 K relative to baseline established on 1951–1980 average temperatures. In order to abate these changes in Earth's atmosphere the international agreements, like the one from Kyoto and COP21 [5, 6], about decreasing emissions of greenhouse gases are implemented. Their goal is to mitigate consequences or to even prevent climate from further changes.

Environment restrictions require reducing carbon dioxide emission. Removal of CO_2 may be performed by, for instance, membrane separation [7], cryogenic method [8], or solid or liquid sorbents [9–12]. Those methods may be implemented for capturing carbon dioxide from precombustion, postcombustion, oxyfuel combustion, and chemical looping combustion [13]. Postcombustion method is crucial for conventional power plants using fossil fuels. It requires solid state adsorbents or liquid absorbents. The most common liquid absorbents are amines [14]. Nevertheless, those chemicals are toxic and corrosive, may decompose during regeneration step, and are dangerous for the environment. Any leakage may lead to serious consequences in nature surrounding the installation. Therefore, to prevent possible drawbacks of liquid absorbents, the solid adsorbents, especially carbonaceous materials, are possible alternatives [15]. Activated carbons, depending of the source of a precursor, may contain inorganic matter, also known as ash [16, 17]. The inorganic matter content in activated carbons due to its variety and complexity

greatly impedes understanding of phenomena responsible for CO_2 sorption. On the other hand, carbon nanotubes are extremely pure and well defined materials containing tiny amounts of catalyst, which may be removed in simple acid treatment with hydrochloric acid [18]. Therefore the MWCNT may be used as a model material, helpful for explanation of effects occurring during modification. There are many comprehensive research papers about modification of multiwalled carbon nanotubes, for instance, impregnating them with amines [19, 20]. Some of them use two-step method, including as a first step of oxidizing with a nitric acid or a mixture of nitric and sulfuric acids. However, those oxidized materials are usually not fully characterized; thus changes of material properties cannot be properly understood and explained.

This research paper consists of preparation of carbon dioxide adsorbent based on multiwalled carbon nanotubes and its characterization. Modification was performed by treating raw material with both oxidizing agents: nitric acid and a mixture of sulfuric and nitric acids. The aim of this paper was to emphasize changes occurring during oxidation of multiwalled carbon nanotubes by evaluation of pore size distributions from nitrogen adsorption/desorption isotherms at 77 K and carbon dioxide adsorption/desorption isotherms at 273 K. Both distributions were evaluated by a density functional theory method (DFT). Enhanced CO_2 sorption capacity was correlated with increased volume of micropores below diameter of 0.8 nm. We strongly believe that all presented results combined will be useful for other research teams interested in carbon nanotubes and environmental chemistry.

2. Materials and Methods

2.1. Chemicals and Materials. Commercial multiwalled carbon nanotubes obtained from Sigma Aldrich, (724769 ALDRICH, CAS number 308068-56-6) were chosen as a starting material for the preparation of CO_2 adsorbents. These nanotubes were prepared by chemical vapor deposition (CVD) using cobalt and molybdenum as catalyst (CoMoCAT). Nitric acid (65% p.a., CHEMPUR) and sulfuric acid (95% p.a., CHEMPUR) were used for the modification.

CO_2 uptake measurements were performed with high purity carbon dioxide (5.0, Air Liquide, Poland).

2.2. Experimental. 200 mg of pristine material was placed in round-bottom flask with three necks (each neck with ground glass joint). 25 ml of concentrated nitric acid was added dropwise via a dropping funnel. Mixture was stirred on a magnetic stirrer under reflux at 373 K for 6 hours. Temperature controller was used for keeping stable temperature during the process. Thermocouple type K was placed in a glass pipe (outer diameter of 5 mm) with one end sealed in the acid. The second end was placed tight in the neck. After the oxidation, sample was washed up to ~7 pH and dried under vacuum at 373 K overnight. The same procedure was used with a mixture of concentrated nitric and concentrated sulfuric acid ($V_{HNO3} : V_{H2SO4}$ 1 : 3). Starting, unmodified material will be further referred to in this paper as CNT_pristine and modified samples will be referred to as "CNT" followed by name of acid used for this particular treatment. For instance, carbon nanotubes after nitric acid treatment will be referred to as CNT_HNO_3.

2.3. Methods. Specific surface area (SSA) was measured by N_2 adsorption-desorption isotherm measurement at 77 K and relative pressure up to 0.99 *(Quantachrome; Autosorb Instrument)*. SSA was calculated using the Brunauer-Emmett-Teller (BET) equation. The total pore volume (V_{total}), including micro-, meso-, and some macropores of specific diameters, was estimated from the amount of nitrogen adsorbed at the highest P/P_0 ratio. Quenched solid density functional theory (QSDFT) based on N_2 adsorption/desorption isotherms for the cylindrical pore model was used to determine pore size distributions (PSD) and micropore volume (V_{micro}) for pores up to 2 nm diameter. Before the analysis, samples were degassed at 373 K under vacuum for 16 h.

Carbon dioxide sorption capacity was measured at 273 K and relative pressure up to 0.95 in a volumetric apparatus (Quadrasorb SI Automated Surface Area & Pore Size Analyzer; *Quantachrome Instruments*). Nonlocal density functional theory (NLDFT) based on CO_2 adsorption/desorption isotherms was used to determine PSD and $V_{submicro}$ for pores up to 0.8 nm diameter. Before the analysis, samples were degassed at 373 K under vacuum for 16 h.

Chemical composition was performed via X-ray photoelectron spectroscopy analysis. Measurements were performed in a commercial multipurpose (AES, UPS, LEED, XPS) UHV surface analysis system *(PREVAC)*. The system includes two chambers for preparation and analysis. The analysis chamber is equipped with nonmonochromatic X-ray photoelectron spectroscopy and kinetic electron energy analyzer (SES 2002; *Scienta*). The calibration of the spectrometer was performed using Ag $3d_{5/2}$ transition. Prior to the measurement samples were degassed. The XPS analysis was performed using Al K_α (h = 1489.6 eV) radiation. The small charging effects were corrected via attribution of carbon peak C 1s to 284.6 eV binding energy. The charge correction using C 1s signal is the standard procedure as traces of carbon are commonly present in typical samples under vacuum conditions [28].

Diameters of the carbon nanotubes were measured via high-resolution transmission electron microscope (HRTEM) operating at 200 kV *(FEI, Tecnai F20)*. Samples were prepared by drop casting diluted suspension onto copper grids and dried at room temperature for 24 h.

3. Results and Discussion

3.1. Textural Characterization. Table 1 presents textural parameters obtained with BET method and CO_2 sorption capacity. N_2 adsorption/desorption isotherms of all samples are presented in Figure 1 (adsorption isotherm is indicated by a curve with filled objects and desorption isotherm is indicated by a curve with blank objects). These isotherms exhibit a type V shape for two modified samples and type V shape with continuous adsorption at $P/P_0 \approx 1$, for pristine material. Type V isotherms are characteristic for porous material with dominating mesopores. Type V was assigned

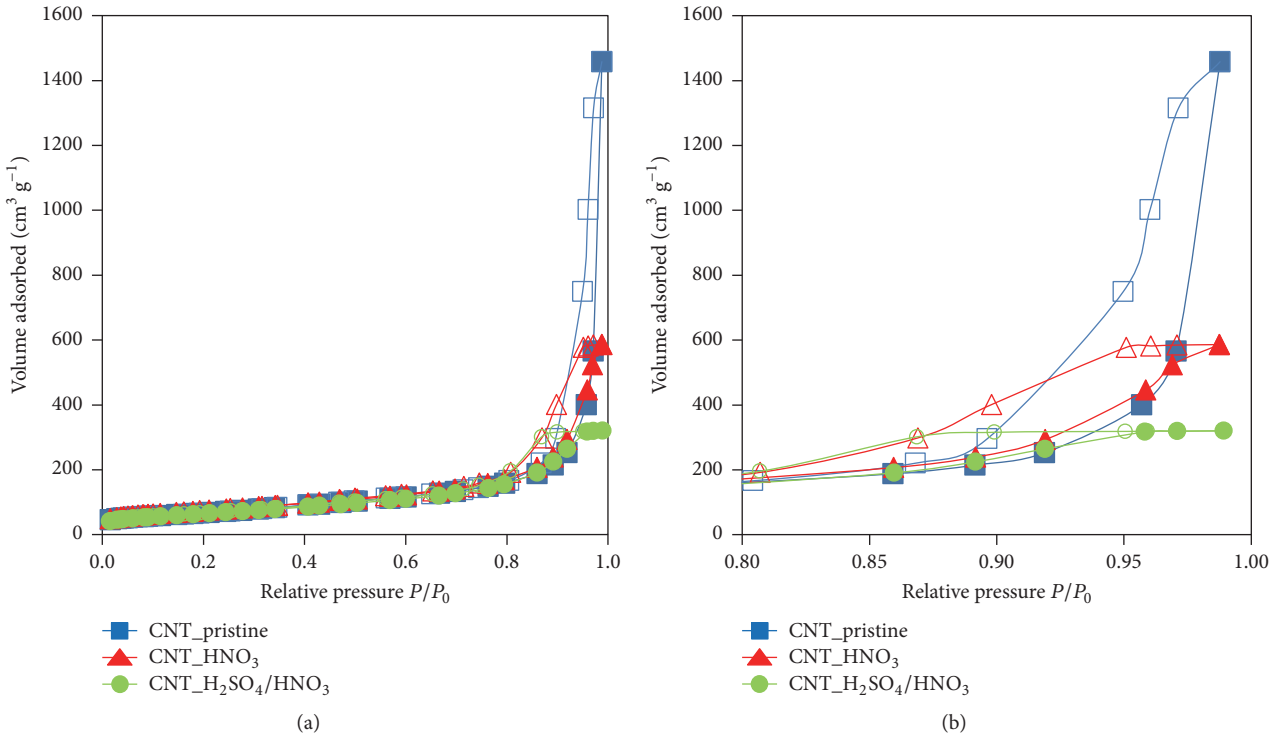

FIGURE 1: N_2 adsorption/desorption isotherms of pristine and modified multiwalled carbon nanotubes: (a) presenting isotherms in full range and (b) presenting only range P/P_0 0.80–1.00 for better insight in changes of isotherms.

TABLE 1: BET and CO_2 sorption capacity results of pristine and modified samples.

Sample	SSA [$m^2 g^{-1}$]	CO_2 uptake [mmol g^{-1}]	V_{total} [$cm^3 g^{-1}$]	V_{micro} [$cm^3 g^{-1}$]	$V_{submicro}$ [$cm^3 g^{-1}$]
CNT_pristine	240	1.74	2.26	0.02	0.10
CNT_HNO$_3$	265	2.28	0.91	0.02	0.11
CNT_H$_2$SO$_4$/HNO$_3$	233	2.53	0.50	0.02	0.13

according to IUPAC. A hysteresis loop in higher relative pressure values may indicate capillary condensation phenomena in mesopores.

Modification led to changes in specific surface area. An increase of SSA for CNT_HNO$_3$ and a decrease for CNT_H$_2$SO$_4$/HNO$_3$ was observed. It was reported by other research papers [21, 22] that oxidizing of the carbon nanotubes may lead to removing impurities and cutting nanotubes and/or opening their ends, resulting in an increase of SSA. However, oxidizing of the MWCNT may lead to formation of defect structures resulting in a significant decrease of SSA, as stated in [23] from 236 m^2/g to 2 m^2/g. The highest obtained specific surface area does not correlate with the highest sorption capacity. This phenomenon will be explained later in this paper. Table 2 presents papers about oxidation of multiwalled carbon nanotubes and its impact on specific surface area.

Presented papers prove that SSA of MWCNT may increase after oxidation step. Of course, it is possible for specific surface area to decrease, due to high oxidation and compaction of the sample, as reported in [23], but it was not observed in our research.

Changes of macropore and submicropores volume are observed. The total pore volume (V_{total}) of the samples CNT_pristine, CNT_HNO$_3$, and CNT_H$_2$SO$_4$/HNO$_3$ was obtained for pores smaller than 158.8 nm, 156.0 nm, and 180.6 nm, respectively. One can notice that V_{total} is being reduced in each treatment; thus it decreases the volume of macropores. On the other hand, Table 1 also presents submicropore volume for pores diameter up to 0.8 nm calculated from CO_2 adsorption/desorption isotherms at 273 K. Pore size distributions for all samples were presented in Figure 2. DFT and BJH methods were used to compare results. As it may be seen, both methods indicate for sample CNT_H$_2$SO$_4$/HNO$_3$ disappearing of pores above diameter of ~15 nm. However, due to DFT versatile use for microporous and mesoporous materials, we believe that PSD in Figure 2(a) is in agreement with actual pores structure. Furthermore, DFT is considered as a better method of analyzing nanopores than BJH, as stated in [29]. On the other hand, BJH method

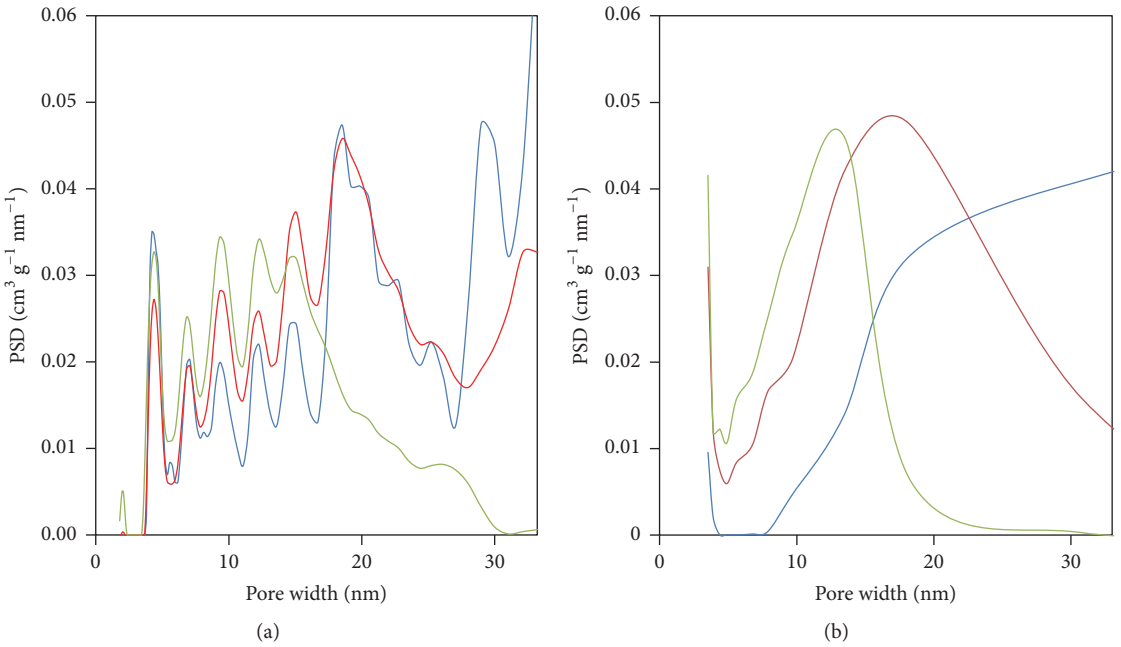

Figure 2: Pore size distributions evaluated by methods: (a) DFT and (b) BJH. Lines present the following samples: blue—CNT_pristine, red—CNT_HNO_3, and green—CNT_H_2SO_4/HNO_3. Both PSD were calculated from N_2 adsorption/desorption isotherms at 77 K.

Table 2: Literature review about oxidation of carbon nanotubes.

Reference	Material	Oxidizing agent	Concentration or ratio	Time of the oxidation [h]	Temperature of the oxidation [K]	SSA [m^2/g]
This research	MWCNT	Pristine	—	—	—	240
		HNO_3	Concentrated	6	373	265
		HNO_3/H_2SO_4	1 : 3	6	373	233
[21]	MWCNT	Pristine	—	—	—	162
		HNO_3	Concentrated	1	413	225
				2	413	237
				6	413	243
				10	413	195
[22]	MWCNT	Pristine	—	—	—	109
		HNO_3/H_2SO_4	1 : 3	12	353	127
[23]	SWCNT	Pristine	—	—	—	236
		HNO_3	3M	45	Not listed	2
[24]	Carbon nanofibers	Pristine	—	—	—	137
		HNO_3	Concentrated	0.5	Boiling point	156
				2	Boiling point	186
		HNO_3/H_2SO_4	1 : 1	0.5	Boiling point	183
			1 : 3	0.5	Boiling point	194
[25]	MWCNT	Pristine	—	—	—	120
		HNO_3/H_2SO_4	1 : 3	1.5	363	116
[26]	MWCNT	Pristine	—	—	—	109
		HNO_3/H_2SO_4	0.6	24	Not listed	179

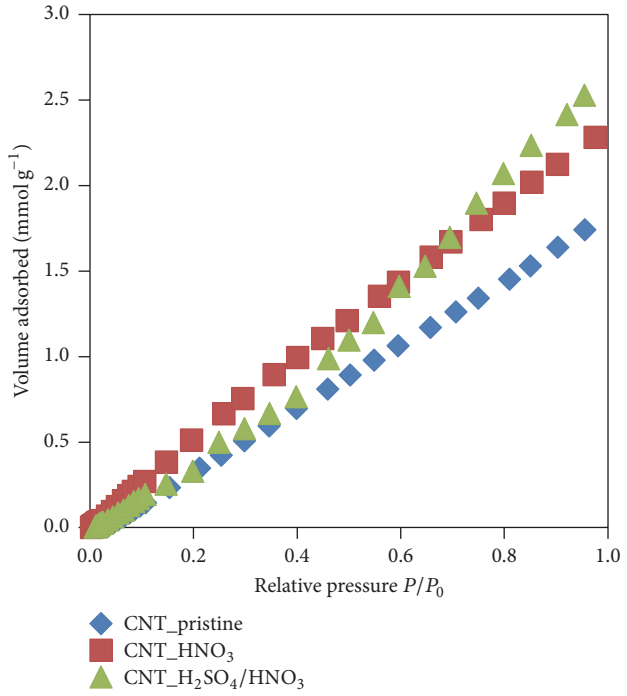

Figure 3: Carbon dioxide adsorption isotherms of pristine and modified multiwalled carbon nanotubes.

may be used for evaluating PSD for pores with higher diameter than 30 nm, thus presenting results for whole mesoporous structure. It is clearly visible that larger mesopores disappear, on the benefit of increasing volume of smaller mesopores and even pores with diameter of 2 nm, which could be classified as micropores. It is well established that the increase of submicropore volume enhances CO_2 uptake [30–33]. The submicropore volume increases significantly in modified samples compared to pristine material, that is, by 10 and 30%.

One can notice an apparent discrepancy; that is, submicropore volume of pore width up to 0.8 nm is larger for each sample than micropore volume of pores to 2 nm. The reason why there is such a difference is related to limitations of used methods. The submicropore volume is determined by CO_2 sorption. Carbon dioxides at 273 K penetrate micropores (smaller than 2 nm) much more efficiently than nitrogen at 77 K. CO_2 adsorption/desorption isotherms allow determining pore size distribution up to about 1.5 nm. On the other hand, N_2 adsorption/desorption isotherms allow determining pore size distribution from about 1.5 nm. Thus, each method covers some range of pore diameters without the possibility of detecting other diameters. In other words the CO_2 sorption method is blind for pores bigger than 1.5 nm and N_2 sorption method is blind for pores smaller than 1.5 nm.

3.2. CO_2 Adsorption. CO_2 adsorption isotherms are presented in Figure 3. It was revealed that both acid treatments led to enhancement of carbon dioxide sorption capacity. The highest enhancement can be observed for multiwalled carbon nanotubes after modification with mixture of nitric

Table 3: XPS results of the surface of multiwalled carbon nanotubes.

Sample	Concentration [at. %]		
	C	O	N
CNT_pristine	96.23	3.77	—
CNT_HNO$_3$	91.23	8.36	0.42
CNT_H$_2$SO$_4$/HNO$_3$	89.03	10.41	0.57

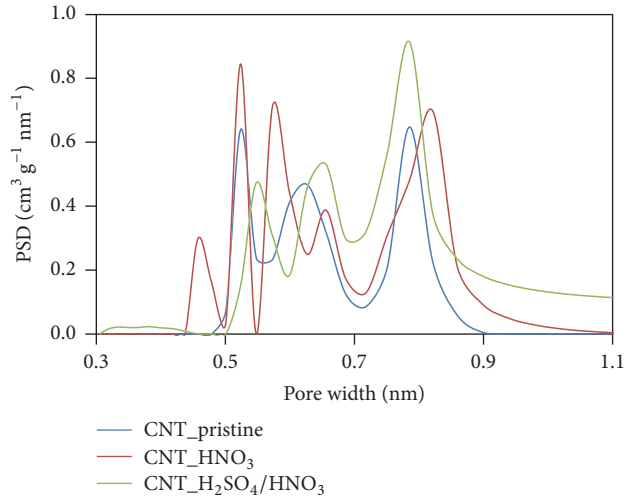

Figure 4: Pore size distributions of pristine and modified multiwalled carbon nanotubes calculated from CO_2 adsorption/desorption isotherms at 273 K.

and sulfuric acids. However, sample CNT_H$_2$SO$_4$/HNO$_3$ has the lowest total pore volume, due to a significant reduction of macropores and increased volume of smaller mesopores and micropores. Thus, all these changes may influence CO_2 sorption enhancement.

Figure 4 presents pore size distributions for pristine and modified samples. Micropores, especially up to 0.8 nm, are crucial for the CO_2 sorption capacity, due to accessibility of those pores for carbon dioxide particles [34]. Volume of this pores increased after both acid treatments, which correlates with increase of CO_2 uptakes presented in Table 1.

3.3. XPS Analysis. X-ray photoelectron spectroscopy was performed to analyze the chemical composition of carbon nanotubes. Obtained results are presented in Table 3.

Both acid treatments introduce oxygen and nitrogen to the carbon nanotubes, with the highest oxygen and nitrogen content for the sample after modification with a mixture of nitric and sulfuric acids.

Table 4 presents results of oxidation ratio from other research papers.

There are reports in literature about high oxidation after mild nitric acid treatment. However, results presented in this paper are similar to some already reported in other research papers. As it may be noticed, oxidation of carbon nanofibers in concentrated acid for 2 hours resulted in O/C ratio lower than our sample CNT_HNO$_3$ treated for 6 hours.

Table 4: Oxidation results from literature.

Reference	Material	Oxidizing agent	Time of the oxidation step [h]	Temperature of the oxidation step [K]	Oxidation ratio at.% O : at.% C
This research	MWCNT	Pristine	—	—	0.011
		HNO_3	6	373	0.080
		HNO_3/H_2SO_4	6	373	0.092
[24]	CNF	Pristine	—	—	0.016
		Conc. HNO_3	2	Not stated	0.069
[27]	MWCNT	Pristine	—	—	0.012
		4M HNO_3/H_2SO_4	12	Boiling point	0.024
		4M HNO_3/H_2SO_4	24	Boiling point	0.072
		4M HNO_3/H_2SO_4	48	Boiling point	0.078
		4M HNO_3/H_2SO_4	96	Boiling point	0.096
		4M HNO_3/H_2SO_4	168	Boiling point	0.107

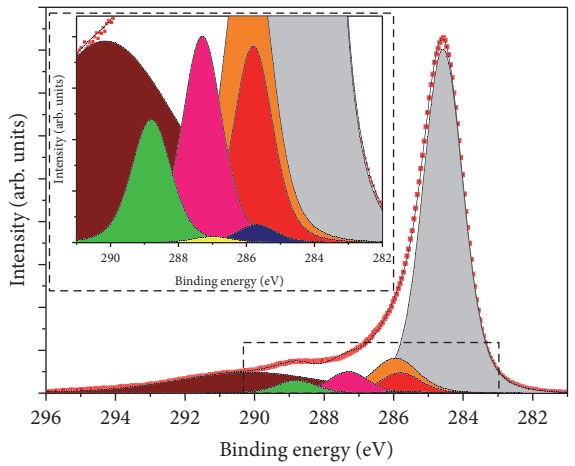

Figure 5: Deconvoluted C 1s signal for CNT_H_2SO_4/HNO_3 sample. Each filling indicates another component: grey—sp^2 carbon (graphite like), orange—sp^3 carbon (defects), red—C-O, pink—C=O, green—COOH, blue—sp^2 carbon with nitrogen, yellow—sp^3 carbon with nitrogen, and brown—satellite. Red squares indicate experimental data and black line indicates an envelope.

Oxidation of MWCNT in mild solution of a mixture of HNO_3/H_2SO_4 at boiling point resulted in similar results for our CNT_H_2SO_4/HNO_3 only after 4 days. It seems that time of the process is crucial.

Deconvolution of C 1s, O 1s, and N 1s signals was performed for sample CNT_H_2SO_4/HNO_3 and it was presented in Figures 5, 6(a), and 6(b), respectively. In case of C 1s signal the following functional groups were identified [35–37]: graphite (sp^2 C) 284.6 ± 0.3 eV, carbon in defects (sp^3 C) 285.5 eV, C=N 285.8 ± 0.1 eV, C-N 287.1 ± 0.1 eV, C=O 287.6 ± 0.3 eV, C-O 286.1 ± 0.3 eV, COOH 289.1 ± 0.3 eV, and satellite 292.15 ± 2.15 eV (determined experimentally). FWHM (full width at half maximum) was set at the same value for each component, due to the same transition, except satellite.

Table 5: The content of C 1s constituents.

Component	CNT_pristine	CNT_HNO_3	CNT_H_2SO_4/HNO_3
Graphite	0.797	0.770	0.776
Defects	0.097	0.111	0.099
sp^3 C-N	0.000	0.001	0.002
sp^2 C=N	0.000	0.003	0.005
C=O	0.035	0.046	0.046
C-O	0.055	0.043	0.044
COOH	0.016	0.025	0.028

In case of O 1s signal the following functional groups were identified [35, 38]: NO_2, C=O 531.1 ± 0.3 eV, C-O 532.8 ± 0.5 eV, and COOH 534.2 ± 0.3 eV. FWHM was set at the same value for each component, due to the same transition.

According to [39, 40], the following components were used for a deconvolution of N 1s signal: C-N-C (pyrrolic-N) 400.4 ± 0.3 eV, N-$(C)_3$ (graphitic nitrogen) 401.4 ± 0.3 eV, and NO_2 ~406 eV. Nitrogen signal is divided into two separate peaks. The left one, at higher binding energies, may be associated with NO_2 group, due to binding nitrogen with more electronegative oxygen. One can notice that the right peak, at binding energies 400–402 eV, is asymmetric and thus composed of at least two components. The component B1 should be associated with pyrrolic nitrogen and the component B2 with graphitic nitrogen.

C 1s signal for raw and after acid treatment samples was normalized and presented in Figure 7. Normalization was performed to emphasize the differences in signal shape. Both modifications with acids led to appearance of a higher shoulder on the left side of the main peak compared to pristine material. Constituents in this particular shoulder are based on carbon-oxygen and carbon-nitrogen bonds, like those presented in deconvoluted signal in Figure 5. To determine changes in constituents content, all C 1s signals for raw and modified samples were deconvoluted and results are presented in Table 5. As it may be seen, content of functional groups containing oxygen increases after modification with

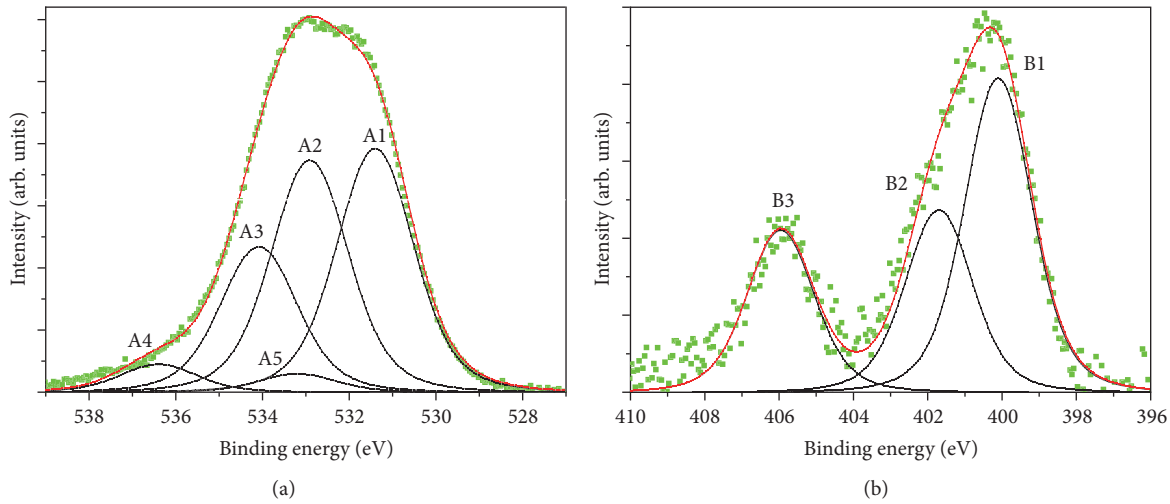

FIGURE 6: Deconvoluted signals: (a) O 1s and (b) N 1s. Abbreviations stand for following components: A1—C=O, A2—C-O, A3—COOH, A4—H_2O, A5—NO_2, B1—C-N-C (pyrrolic-N), B2—N-$(C)_3$ (graphitic nitrogen), and B3—NO_2.

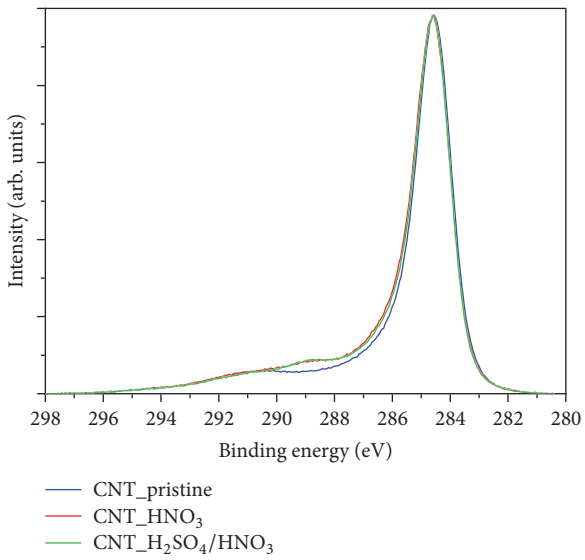

FIGURE 7: Normalized C 1s signals for pristine and modified samples.

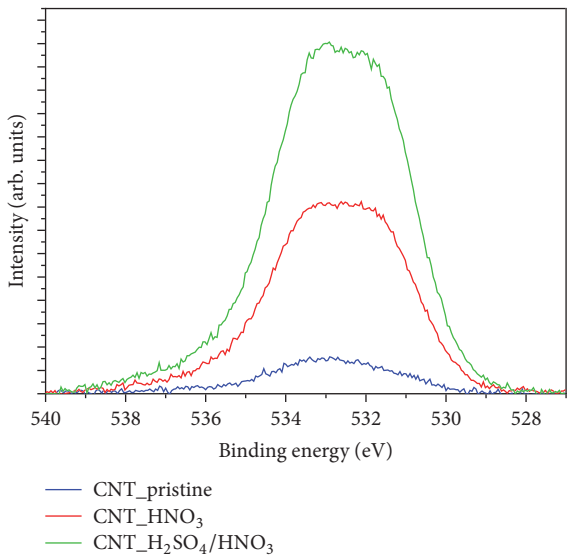

FIGURE 8: O 1s signals for pristine and modified samples.

acids. Thus, it confirms increased oxygen concentration in multiwalled carbon nanotubes and confirms graphite content decrease. The functional groups containing nitrogen are introduced to the structure of CNT. Those constituents influence shapes of C 1s signal as it was mentioned before. Nevertheless, deconvolution of C 1s is a very difficult task, due to presence of few possible components with similar binding energies.

Nitric acid and a mixture of nitric and sulfuric acids are well known for their oxidizing properties. Figure 7 contains results of an impact on C 1s signal of oxidizing the material. Figure 8 presents intensity changes of O 1s signal, which correlate with data in Table 3. It may be observed that both treatments introduce the oxygen to carbon nanotubes, with the highest content for the sample CNT_H_2SO_4/HNO_3.

Functional groups are responsible for chemical character of samples surface. Acidity is closely associated with the oxygen groups, like those from Table 5 [41]. As it may be seen, their content increases after treatment. On the other hand, basicity may be related to resonating π-electrons of carbon aromatic rings, which attract protons and basic surface functionalities, for instance, functional groups containing nitrogen [41]. Moreover, the acids treatment through oxidation may open the ending of MWCNT [42] and may create intercalates, that is, increase of the distances between graphitic layers. This may lead to increase of submicropore volume which is crucial for CO_2 uptake. CO_2 sorption capacity for all samples will be an overall result of those two effects.

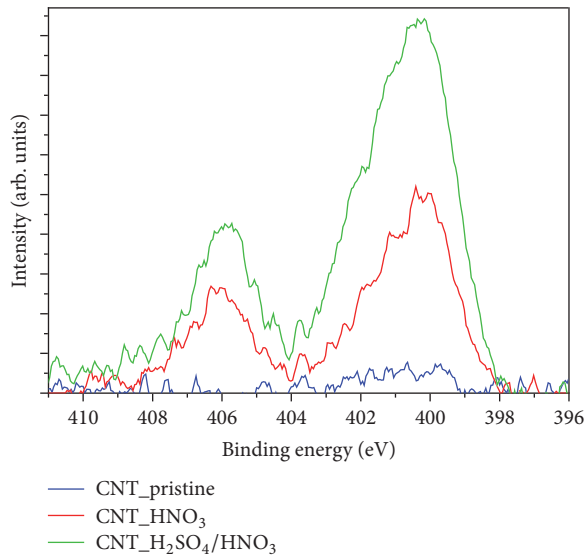

Figure 9: N 1s signals for modified samples.

Table 6: Diameters with standard deviations of pristine and modified multiwalled carbon nanotubes.

Sample	Average diameter [nm]	Standard deviation
CNT_pristine	14.5	5.6
CNT_HNO_3	13.8	4.4
CNT_H_2SO_4/HNO_3	15.7	2.7

Figure 9 presents comparison of N 1s signals for samples CNT_pristine, CNT_HNO_3, and CNT_H_2SO_4/HNO_3. We believe that nitrogen in pristine sample was below the detection limit; thus Figure 9 presents only noise for CNT_pristine. As it may be noticed, oxidizing material with a mixture of HNO_3 and H_2SO_4 resulted in higher nitrogen content in the structure of multiwalled carbon nanotubes.

3.4. TEM Results. TEM images presented in Figure 10 confirm the typical multiwalled carbon nanotubes structure of pristine material. Figure 10(a) presents a clear fragment of this single structure with multiple walls of nanotubes and its empty center. Micrographs in Figures 10(b), 10(c), and 10(d) were used to perform statistical analysis of CNT diameters. Based on average of 33 diameters' measurements it was observed that they exhibit normal distribution. Therefore they can be described with two parameters, that is, an average diameter and standard deviation. Results are presented in Table 6 and normal distributions are presented in Figure 11.

One can notice that acid treatment leads to slight yet observable change of average diameter of CNT. Moreover the content of CNT of small diameter is lower after acid treatment. The possible mechanism of observed phenomenon may be oxidation of carbon in external layers of MWCNT to CO and/or to CO_2, resulting in smaller average diameter than pristine material. However, this mechanism applies to all CNT during the process; thus wider nanotubes are being narrowed and narrow nanotubes may disappear during the process of oxidation. This is in an agreement with data presented in Figure 11. Sample CNT_H_2SO_4/HNO_3 has narrower normal distribution than sample CNT_pristine, which proves mentioned mechanism. Similar results were observed as well in [43].

As reported in [44], a decrease of carbon nanotube diameter leads to an increase of specific surface area. It can be expected that an increase of CNT diameter leads to a decrease of SSA. Experimental data presented in the paper proves this report from literature. Sample CNT_HNO_3 has lower average diameter than pristine material and higher SSA – 240 m^2/g for pristine material and 265 m^2/g for CNT_HNO_3. On the other hand, sample CNT_H_2SO_4/HNO_3 has SSA of 233 m^2/g and higher average diameter.

4. Conclusions

Multiwalled carbon nanotubes may be used as a simple model carbon structure for investigation of modification effects of other more complex carbon-based adsorbents. Treating MWCNT with oxidizing acids led to an increased CO_2 sorption capacity. An 31% and 45% sorption enhancement for nitric acid and a mixture of nitric and sulfuric acids was observed, respectively. The sorption enhancement occurs despite the fact that those treatments have increased acidity by introducing acidic functional groups to the surface of materials as confirmed by XPS. The CO_2 enhancement is attributed to increase of the pore volume of submicropores. The decrease of macropores was observed which is believed to have no impact on CO_2 sorption. However this effect may be useful in obtaining more compact and dense materials. Oxidizing of carbon nanotubes led to changes in their diameters distributions. Pristine MWCNT have wide range of diameters. Each modification led to narrower distribution

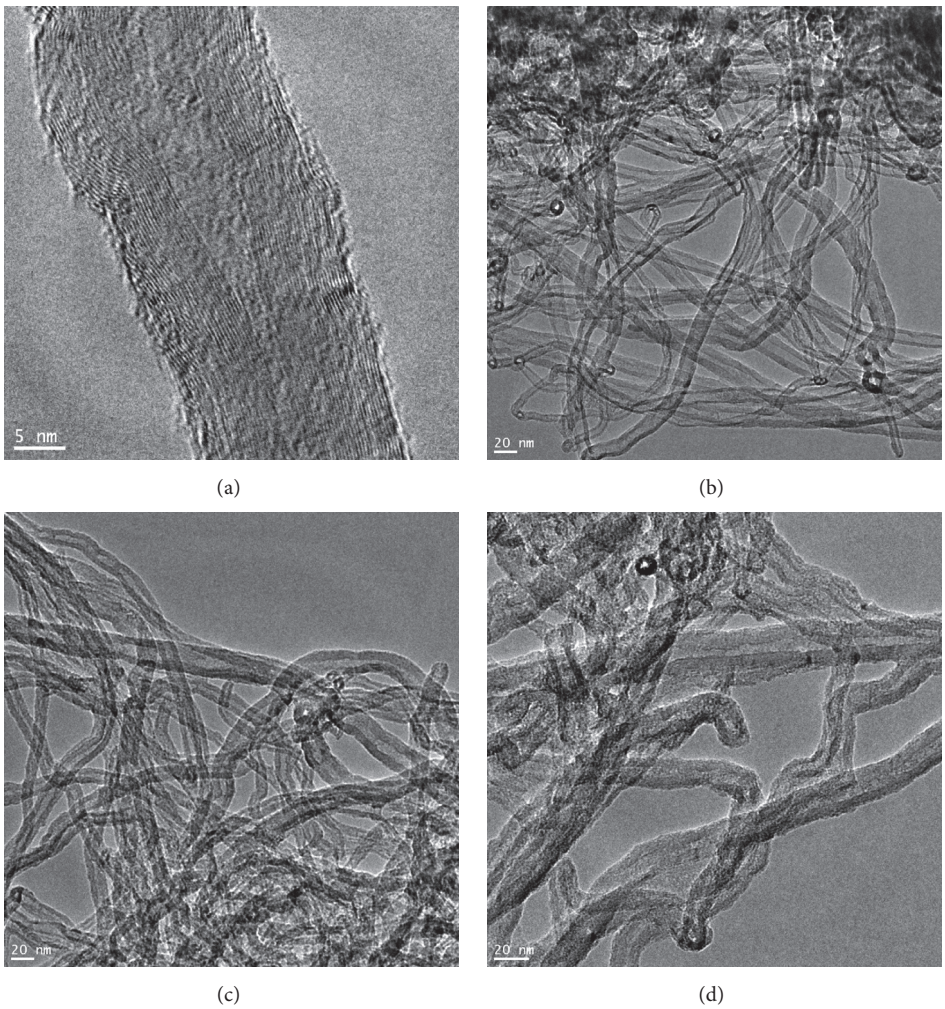

Figure 10: TEM micrographs: (a) and (b) CNT_pristine, (c) CNT_HNO_3, and (d) CNT_H_2SO_4/HNO_3.

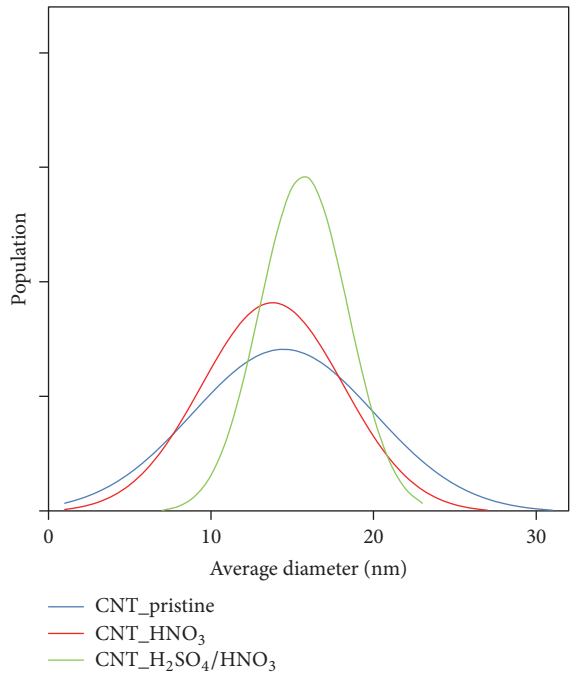

Figure 11: Normal distributions of average diameters of pristine and modified multiwalled carbon nanotubes.

than starting material, increasing occurrence of medium (~15 nm) diameters.

XPS analysis confirmed oxidizing of the material, due to an increase of oxygen concentration, and confirmed presence of nitrogen functional groups on the surface.

Conflicts of Interest

The authors declare that there are no conflicts of interest regarding of publication of this article.

Acknowledgments

The research leading to these results has received funding from the Polish-Norwegian Research Programme operated by the National Centre for Research and Development under the Norwegian Financial Mechanism 2009–2014 in the frame of Project Contract no. Pol-Nor/237761/98.

References

[1] D. L. Hartmann, A. M. G. Klein Tank, M. Rusticucci, L. V. Alexander, S. Bronnimann, Y. Charabi et al., "Observations: Atmosphere and Surface," in *Climate Change 2013: The Physical Science Basis. Contribution of Working Group I to the Fifht Assessment Report of the Intergovernmental Panel on Climate Change*, pp. 159–254, Cambridge University Press, Cambridge, UK, 2013.

[2] E. Dlugokencky and P. Tans, NOAA/ESRL. http://www.esrl.noaa.gov/gmd/ccgg/trends/.

[3] D. M. Etheridge, L. P. Steele, R. L. Langenfelds, R. J. Francey, J.-M. Barnola, and V. I. Morgan, "Natural and anthropogenic changes in atmospheric CO_2 over the last 1000 years from air in Antarctic ice and firn," *Journal of Geophysical Research Atmospheres*, vol. 101, article 95JD03410, no. 2, pp. 4115–4128, 1996.

[4] http://climate.nasa.gov/vital-signs/global-temperature/.

[5] C. Almer and R. Winkler, "Analyzing the effectiveness of international environmental policies: The case of the Kyoto Protocol," *Journal of Environmental Economics and Management*, vol. 82, pp. 125–151, 2017.

[6] "Adoption of the Paris Agreement (FCCC/CP/2015/L.9/Rev.1)," United Nations Framework Convention on Climate Change, Paris, 2015.

[7] M. J. Tuinier, H. P. Hamers, and M. Van Sint Annaland, "Techno-economic evaluation of cryogenic CO2 capture-A comparison with absorption and membrane technology," *International Journal of Greenhouse Gas Control*, vol. 5, no. 6, pp. 1559–1565, 2011.

[8] A. Hart and N. Gnanendran, "Cryogenic CO2 capture in natural gas," in *Proceedings of the 9th International Conference on Greenhouse Gas Control Technologies, GHGT-9*, pp. 697–706, usa, November 2008.

[9] Y. Liang, D. P. Harrison, R. P. Gupta, D. A. Green, and W. J. McMichael, "Carbon dioxide capture using dry sodium-based sorbents," *Energy and Fuels*, vol. 18, no. 2, pp. 569–575, 2004.

[10] D. P. Hagewiesche, S. S. Ashour, H. A. Al-Ghawas, and O. C. Sandall, "Absorption of carbon dioxide into aqueous blends of monoethanolamine and N-methyldiethanolamine," *Chemical Engineering Science*, vol. 50, no. 7, pp. 1071–1079, 1995.

[11] S. Kim, H. Shi, and J. Y. Lee, "CO2 absorption mechanism in amine solvents and enhancement of CO2 capture capability in blended amine solvent," *International Journal of Greenhouse Gas Control*, vol. 45, pp. 181–188, 2016.

[12] J. Kapica-Kozar, E. Kusiak-Nejman, A. Wanag et al., "Alkali-treated titanium dioxide as adsorbent for CO2 capture from air," *Microporous and Mesoporous Materials*, vol. 202, no. C, pp. 241–249, 2015.

[13] S. A. Rackley, *Carbon Capture and Storage*, Elsevier, Burlington, 2010.

[14] C.-H. Yu, C.-H. Huang, and C.-S. Tan, "A review of CO_2 capture by absorption and adsorption," *Aerosol and Air Quality Research*, vol. 12, no. 5, pp. 745–769, 2012.

[15] C. Lu, H. Bai, B. Wu, F. Su, and J. F. Hwang, "Comparative study of CO_2 capture by carbon nanotubes, activated carbons, and zeolites," *Energy and Fuels*, vol. 22, no. 5, pp. 3050–3056, 2008.

[16] A. Mao, H. Wang, L. Tan, X. Nin, and R. Pan, "Effects of acid treatment on activated carbon used as a support for Rb and K catalyst for C2F5I synthesis and its mechanism," *Journal of Fluorine Chemistry*, vol. 132, no. 8, pp. 548–553, 2011.

[17] A. Gęsikiewicz-Puchalska, M. Zgrzebnicki, B. Michalkiewicz, U. Narkiewicz, A. W. Morawski, and R. J. Wrobel, "Improvement of CO2 uptake of activated carbons by treatment with mineral acids," *Chemical Engineering Journal*, vol. 309, pp. 159–171, 2017.

[18] B. Scheibe, E. Borowiak-Palen, and R. J. Kalenczuk, "Oxidation and reduction of multiwalled carbon nanotubes—preparation and characterization," *Materials Characterization*, vol. 61, no. 2, pp. 185–191, 2010.

[19] F. Su, C. Lu, W. Cnen, H. Bai, and J. F. Hwang, "Capture of CO2 from flue gas via multiwalled carbon nanotubes," *Science of the Total Environment*, vol. 407, no. 8, pp. 3017–3023, 2009.

[20] Q. Liu, Y. Shi, S. Zheng et al., "Amine-functionalized low-cost industrial grade multi-walled carbon nanotubes for the capture of carbon dioxide," *Journal of Energy Chemistry*, vol. 23, no. 1, pp. 111–118, 2014.

[21] H. Wang, A. Zhou, F. Peng, H. Yu, and J. Yang, "Mechanism study on adsorption of acidified multiwalled carbon nanotubes to Pb(II)," *Journal of Colloid and Interface Science*, vol. 316, no. 2, pp. 277–283, 2007.

[22] O. A. Oyetade, A. A. Skelton, V. O. Nyamori, S. B. Jonnalagadda, and B. S. Martincigh, "Experimental and DFT studies on the selective adsorption of Pb 2+ and Zn 2+ from aqueous solution by nitrogen-functionalized multiwalled carbon nanotubes," *Separation and Purification Technology*, vol. 188, pp. 174–187, 2017.

[23] M. T. Martínez, M. A. Callejas, A. M. Benito et al., "Sensitivity of single wall carbon nanotubes to oxidative processing: Structural modification, intercalation and functionalisation," *Carbon*, vol. 41, no. 12, pp. 2247–2256, 2003.

[24] M. L. Toebes, J. M. P. Van Heeswijk, J. H. Bitter, A. Jos van Dillen, and K. P. De Jong, "The influence of oxidation on the texture and the number of oxygen-containing surface groups of carbon nanofibers," *Carbon*, vol. 42, no. 2, pp. 307–315, 2004.

[25] H. Hu, T. Zhang, S. Yuan, and S. Tang, "Functionalization of multi-walled carbon nanotubes with phenylenediamine for enhanced CO2 adsorption," *Adsorption*, vol. 23, no. 1, pp. 73–85, 2017.

[26] A. Policicchio, D. Vuono, T. Rugiero, P. De Luca, and J. B. Nagy, "Study of MWCNTs adsorption performances in gas processes," *Journal of CO2 Utilization*, vol. 10, pp. 30–39, 2015.

[27] Y.-C. Chiang, W.-H. Lin, and Y.-C. Chang, "The influence of treatment duration on multi-walled carbon nanotubes functionalized by H_2SO_4/HNO_3 oxidation," *Applied Surface Science*, vol. 257, no. 6, pp. 2401–2410, 2011.

[28] R. J. Wrobel and S. Becker, "Carbon and sulphur on Pd(111) and Pt(111): Experimental problems during cleaning of the substrates and impact of sulphur on the redox properties of CeOχ in the CeOχ/Pd(111) system," *Vacuum*, vol. 84, no. 11, pp. 1258–1265, 2010.

[29] L. Zhang, Y. Xiong, Y. Li et al., "DFT modeling of CO 2 and Ar low-pressure adsorption for accurate nanopore structure characterization in organic-rich shales," *Fuel*, vol. 204, pp. 1–11, 2017.

[30] G. Yin, Z. Liu, Q. Liu, and W. Wu, "The role of different properties of activated carbon in CO2 adsorption," *Chemical Engineering Journal*, vol. 230, pp. 133–140, 2013.

[31] J. Serafin, U. Narkiewicz, A. W. Morawski, R. J. Wróbel, and B. Michalkiewicz, "Highly microporous activated carbons from biomass for CO2 capture and effective micropores at different conditions," *Journal of CO2 Utilization*, vol. 18, 2017.

[32] S. Deng, H. Wei, T. Chen, B. Wang, J. Huang, and G. Yu, "Superior CO_2 adsorption on pine nut shell-derived activated carbons and the effective micropores at different temperatures," *Chemical Engineering Journal*, vol. 253, pp. 46–54, 2014.

[33] A. L. Myers and J. M. Prausnitz, "Thermodynamics of mixed-gas adsorption," *AIChE Journal*, vol. 11, no. 1, pp. 121–127, 1965.

[34] V. Presser, J. McDonough, S.-H. Yeon, and Y. Gogotsi, "Effect of pore size on carbon dioxide sorption by carbide derived carbon," *Energy and Environmental Science*, vol. 4, no. 8, pp. 3059–3066, 2011.

[35] J. L. Figueiredo and M. F. R. Pereira, "The role of surface chemistry in catalysis with carbons," *Catalysis Today*, vol. 150, no. 1-2, pp. 2–7, 2010.

[36] T. Susi, T. Pichler, and P. Ayala, "X-ray photoelectron spectroscopy of graphitic carbon nanomaterials doped with heteroatoms," *Beilstein Journal of Nanotechnology*, vol. 6, no. 1, pp. 177–192, 2015.

[37] V. Datsyuk, M. Kalyva, K. Papagelis et al., "Chemical oxidation of multiwalled carbon nanotubes," *Carbon*, vol. 46, no. 6, pp. 833–840, 2008.

[38] J. Urzúa, J. Carbajo, C. Yáñez, J. F. Marco, and J. A. Squella, "Electrochemistry and XPS of 2,7-dinitro-9-fluorenone immobilized on multi-walled carbon nanotubes," *Journal of Solid State Electrochemistry*, vol. 20, no. 4, pp. 1131–1137, 2016.

[39] D. Liu, X. Zhang, and T. You, "Electrochemical performance of electrospun free-standing nitrogen-doped carbon nanofibers and their application for glucose biosensing," *ACS Applied Materials and Interfaces*, vol. 6, no. 9, pp. 6275–6280, 2014.

[40] S. Kundu, Y. Wang, W. Xia, and M. Muhler, "Thermal stability and reducibility of oxygen-containing functional groups on multiwalled carbon nanotube surfaces: A quantitative high-resolution xps and TPD/TPR study," *Journal of Physical Chemistry C*, vol. 112, no. 43, pp. 16869–16878, 2008.

[41] M. S. Shafeeyan, W. M. A. W. Daud, A. Houshmand, and A. Shamiri, "A review on surface modification of activated carbon for carbon dioxide adsorption," *Journal of Analytical and Applied Pyrolysis*, vol. 89, no. 2, pp. 143–151, 2010.

[42] D. Tasis, N. Tagmatarchis, A. Bianco, and M. Prato, "Chemistry of carbon nanotubes," *Chemical Reviews*, vol. 106, no. 3, pp. 1105–1136, 2006.

[43] K. J. Ziegler, Z. Gu, H. Peng, E. L. Flor, R. H. Hauge, and R. E. Smalley, "Controlled oxidative cutting of single-walled carbon nanotubes," *Journal of the American Chemical Society*, vol. 127, no. 5, pp. 1541–1547, 2005.

[44] D. J. Babu, M. Lange, G. Cherkashinin, A. Issanin, R. Staudt, and J. J. Schneider, "Gas adsorption studies of CO2 and N2 in spatially aligned double-walled carbon nanotube arrays," *Carbon*, vol. 61, pp. 616–623, 2013.